Proceedings of ICRC 2001: 2947 © Copernicus Gesellschaft 2001

ICRC 2001

Gamma ray and hadron generated Čerenkov photon spectra at various observation altitudes

P. Majumdar, B. S. Acharya, P. N. Bhat, V. R. Chitnis, M. A. Rahman, B. B. Singh, and P. R. Vishwanath

Tata Institute of Fundamental Research, Homi Bhabha Road, Mumbai 400005, India

Abstract. Incident Čerenkov photon spectra at various observation altitudes are derived after applying wavelength dependent corrections due to attenuation in the atmosphere during their propagation. These spectra are found to be both altitude and primary energy dependent, the peak of which shifts towards shorter wavelength with increasing altitude of observation for a given primary. Also it shifts towards shorter wavelength with increasing primary energy at a given altitude. The fraction of UV component in this spectrum is estimated both for $\gamma-$ ray and hadron primaries at various observation altitudes and energies. Hadron generated Čerenkov spectra are richer in UV light at higher altitudes. Thus the fraction of UV to visible light in the Čerenkov spectrum could be a useful parameter to separate $\gamma-$ rays from cosmic rays specially at lower primary energies.

1 Introduction

Ground based atmospheric Čerenkov technique is the only method available to date to study VHE $\gamma-$rays from astronomical sources in the energy range of about 100 GeV to few 10's of TeV. (Ong, 1998). In these experiments, $\gamma-$rays from astronomical sources are detected indirectly by detecting Čerenkov light from air showers generated by them. In the absence of standard mono-energetic beams of cosmic rays or $\gamma-$rays, all these experiments make use of simulation techniques extensively to understand and optimize the detector response. We have carried out detailed simulations (Chitnis and Bhat, 1998) with VHE $\gamma-$rays and cosmic rays of various primary energies initiating extensive air showers in the atmosphere using CORSIKA (version 5.62) (Heck et al. 1998). In order to ensure the reliability of the conclusions drawn from these studies it is imperative to verify the correctness of the basic results derived from these simulations.

In the present work, the Čerenkov photon growth curves obtained from the simulations have been compared with those derived from independent empirical relations. The Čerenkov photon spectra as seen at the observation levels are then derived for various primary energies of $\gamma-$rays and protons after taking into account of the wavelength dependent attenuation in the atmosphere. Then we estimate the relative fraction of UV photons in these spectra as a function of primary energy and observation level. We have mainly used Pachmarhi (altitude: 1075 m) as the observer's location where an array of 25 Čerenkov detectors each of area 4.45 m^2 is deployed in the form of a rectangular array (Chitnis et al. 2001). Calculations were also carried out at sea level and a location at an altitude of 2 km above mean sea level.

Correspondence to: pratik@tifr.res.in

2 Calculation of longitudinal profiles

2.1 $\gamma-$ray primaries

For showers initiated by photons of energy E_γ the longitudinal shower development curve is derived from the equation for cascade curve under approximation A. The average number of electrons[1] of all energies $N(E_\gamma, x)$ as a function of atmospheric depth x, is given approximately, in the region where the number of particles is large, by (Greisen, 1956):

$$N(E_\gamma, x) = \frac{0.31}{\sqrt{\ln\left(\frac{E_\gamma}{E_t}\right)}} \exp\left(t(1 - 1.5 \ln s)\right)$$

where t is the depth, x measured in units of radiation length in the atmosphere (37.2 $g\ cm^{-2}$) and E_t is the the electron critical energy at the depth t and has a value 84.2 MeV in air, s is the shower age parameter.(see Rahman et al., 2001).

For calculating the electron growth curve the atmosphere is divided into slabs of thickness 333 m, starting from the first interaction of the primary. The fraction of electrons with energy above the Čerenkov threshold, E_{th}, is given by (Lythe, 1990):

[1]Throughout this paper *electron* implies *electrons* & *positrons*

$$f_{\check{C}} = \left(\frac{0.89E_0 - 1.2}{E_0 + E_{th}}\right)^s (1 + 0.0001sE_{th})^{-2}$$

where E_0 = 26 *MeV* when $s \leq 0.4$
= $44 - 17(s - 1.46)^2$ MeV for $s > 0.4$

The number of electrons above the Čerenkov threshold is then computed in each of the slabs. For each straight section of the electron path, the number of Čerenkov photons produced per unit path-length is given by,

$$\frac{dN}{dl} = 6.28\alpha \left(\frac{1}{\lambda_1} - \frac{1}{\lambda_2}\right)\left(1 - \frac{1}{\beta^2 n^2}\right)$$

in the wavelength band bounded by λ_1 and λ_2 and β is the electron velocity and α is the fine structure constant. Assuming all the electrons in the cascade to be close to the shower axis and they travel with the velocity close to that of light in vacuum, the number of Čerenkov photons produced in a path-length dl (= 333 m) and in the wavelength range 300-550 nm at a depth x $g\ cm^{-2}$ is then given by,

$$N_{ph} = 0.402N \left(\frac{x}{1030}\right) dl$$

2.2 Proton primaries

Because of the differences in the kinematics of shower development in the case of hadronic primaries the longitudinal development profiles too are different as compared to that of $\gamma-$ray primaries. Using the scaling model for nuclear interactions, Gaisser & Hillas (Gaisser and Hillas, 1977) find that the average number of particles, $N(E_p, x)$ at an atmospheric depth of x $g\ cm^{-2}$, measured from the first point of interaction, in a shower initiated by a proton of energy E_p (GeV) can be adequately represented by the empirical relationship (Rao and Sreekantan, 1998; Pyrke, 2000)

$$N(E_p, x) = S_0 \frac{E_p}{\epsilon} e^{t_m} \left(\frac{t}{t_m}\right)^{t_m} e^{-t}$$

where

$$t_m(E_p) = \frac{x_0}{\lambda} \ln\left(\frac{E_p}{\epsilon}\right) - 1$$

where S_0=0.045, ϵ=0.074, x_0= 37.2 $g\ cm^{-2}$, $t = \frac{x}{\lambda}$ and λ =proton interaction mean free path in air (70 $g\ cm^{-2}$). Using the electron energy spectrum given by Zatsepin and Chudakov which is independent of the stage of cascade development (Rao and Sreekantan, 1998; Zatsepin and Chudakov, 1962), the integral electron energy spectrum is given by

$$F(E, x) = 0.75\ N(x)\ \ln\left(1 + \frac{2.3}{\kappa}E\right)$$

Substituting E_{th} for E, the number of electrons above the Čerenkov threshold at a particular depth are calculated.

The longitudinal Čerenkov photon profiles are calculated for $\gamma-$rays of primary energy 50, 100, 250, 500 and 1000 GeV and protons of energy 100, 250, 500, 1000 and 2000 GeV. The growth curves are also simulated using CORSIKA for two primary energies for $\gamma-$rays (500 GeV & 1000 GeV) and protons (1000 & 2000 GeV). Figure 1 shows a comparison of the simulated longitudinal profiles for $\gamma-$ rays (a & c) as well as protons (b & d) with calculated profiles. The simulated profiles (histograms) are averaged over 30 showers for $\gamma-$ rays and 50 showers for protons. The agreement between the two is good. The total number of Čerenkov photons agree within 1 & 2% for $\gamma-$ray and proton primaries respectively.

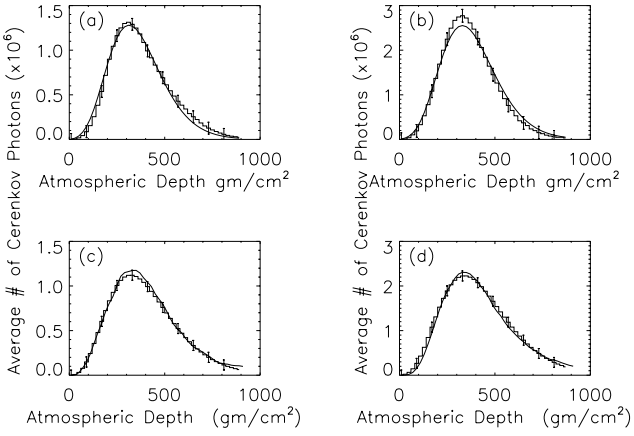

Fig. 1. Čerenkov photon growth curves in the atmosphere for $\gamma-$ ray of (a) 500 GeV & (b) 1 TeV and protons of (c) 1 TeV & (d) 2 TeV primaries. The histograms indicates the simulation results from CORSIKA while the smooth curves indicates the results from analytical calculations.

3 Photon attenuation in the atmosphere

To study the attenuation of Čerenkov light in the atmosphere Elterman's atmospheric attenuation model (Elterman, 1968) is used, which provides the attenuation coefficients for the Rayleigh and aerosol scattering as well as ozone absorption in an altitude dependent form for λ : 270-1260 nm.

The number of photons, integrated over the bandwidth of 300-550 nm (dictated by the photo-tube band-width) and transmitted through a slab (1 km thick) using the corresponding extinction coefficient is given by: $N = N_1 e^{-B}$, where N is the number of photons transmitted through the slab with absorption coefficient B and N_1 is the mean number of photons entering the slab. For each altitude, the photon transmission spectrum is convolved with the Čerenkov photon emission spectrum to get the transmitted spectrum. Showers pass through several such slabs with different transmission coefficients, resulting in a modified longitudinal development profile for the Čerenkov photons that reach the observation level. Figure 2 shows the longitudinal development profiles of Čerenkov photons at production in the atmosphere and that for the photons detected at the observation level for the same wavelength band. From the plots it is clear that the shape of the longitudinal profile remains largely unchanged. The

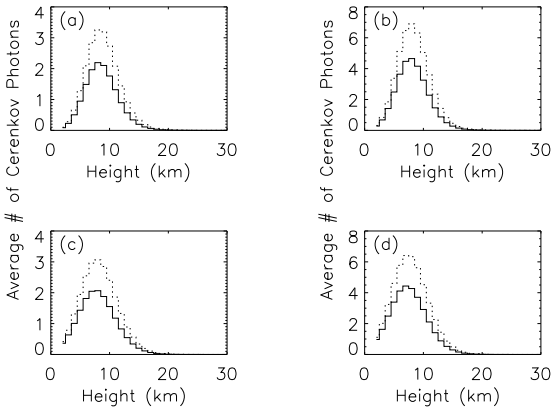

Fig. 2. Longitudinal development profiles of Čerenkov photons at Pachmarhi level with and without atmospheric attenuation correction. a & b are for $\gamma-$ray primaries of energy 50 GeV and 1 TeV respectively while c & d are for proton primaries of energy 100 GeV and 2 TeV respectively (band-width: 300-550 nm).

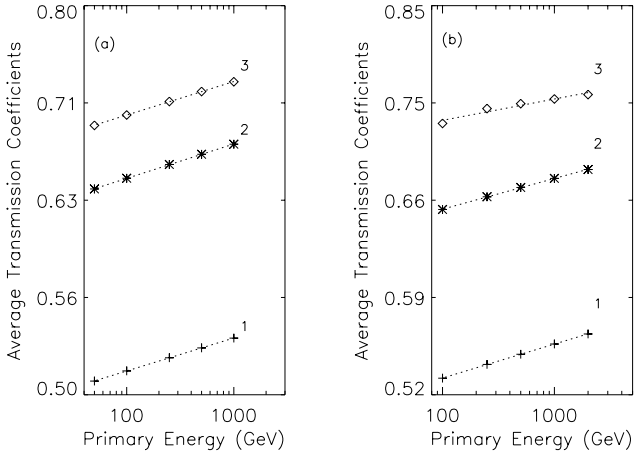

Fig. 3. Average transmission coefficient for Čerenkov photons in the atmosphere for primary (a) $\gamma-$rays and (b) protons of various energies. The straight lines show the fits. The three plots in each panel correspond to three observation levels (1) sea level, (2) Pachmarhi (1 km a.s.l.) and (3) 2 km (a.s.l.) altitude.

range of atmospheric heights from which the detected photons originate also remains unchanged as well, irrespective of the primary energy or species considered. Thus the height of shower maximum remains unchanged due to atmospheric attenuation.

The ratio of the total number of photons within the bandwidth in a shower received at a particular observation level to the total photons produced is defined as the transmission coefficient(T_c). The variation in average T_c for Čerenkov photons in the atmosphere is shown in figure 3 for (a) $\gamma-$ray and (b) protons as a function of primary energy at three different observation levels. T_c is found to vary as a powerlaw in energy for both the species and at all the altitudes.

The increase in T_c with primary energy implies that higher energy primaries penetrate deeper in the atmosphere and hence pass through lesser air mass. The proton primaries reach the shower maximum lower down in the atmosphere compared to a $\gamma-$ray primary of the same energy since the interaction mean free path in air for the former is nearly twice the radiation length. As a result the protons have marginally larger ($\sim 1.2\%$ at 100 GeV to $\sim 0.6\%$ at 1 TeV) average transmission coefficient.

The attenuation of optical photons due to Rayleigh and aerosol scattering is more significant at lower altitudes. As a result the Čerenkov photon transmission is expected to depend on the observation level as also seen in figure 3. The average photon transmission coefficient increases almost linearly with decreasing atmospheric depth and the rate is $\sim 0.1\%$ for every 100 $g\ cm^{-2}$ of air.

4 Čerenkov photon spectrum

The Čerenkov photon spectrum at the observation level is an important input for the design of an atmospheric Čerenkov experiment. The fraction of the photon spectrum bracketed by the photo-multiplier bandwidth has an important bearing on the sensitivity of a TeV $\gamma-$ray telescope. Hence we computed the photon spectrum at different observation levels for $\gamma-$ray and proton primaries of various energies. The bandwidth considered in our calculation is 270-550 nm. Figure 4 shows photon spectra, corresponding to Pachmarhi level, generated by (a) 50 GeV $\gamma-$rays & 100 GeV protons (* & $\diamond$ respectively) as well as (b) 1 TeV $\gamma-$rays & 2 TeV protons. It can be seen from the figure that the wavelength at peak intensity is a function of the primary energy in both the cases. It shifts from around 350 nm at 50 GeV to around 330 nm at 1 TeV. This is because the higher energy primaries reach the shower maximum lower down in the atmosphere compared to lower energy primaries. As a result, absorption of shorter wavelength photons which is primarily due to atmospheric Ozone is comparatively larger for lower energy primaries.

4.1 Fraction of UV component at various altitudes

UV filters were used in some experiments(Goret et al., 1988) for two reasons: firstly, it helps to reduce night sky background while minimizing the loss of Čerenkov light in the blue and near UV range. This would provide better stability at higher photo-tube gains and improve the sensitivity of an experiment. Secondly, it could serve to identify showers with a larger UV fraction in the Čerenkov light. Since the Čerenkov light generated by proton primaries traverse lesser air mass as compared to $\gamma-$ray primaries it is expected to have a larger UV content. This property could be exploited to discriminate against hadronic showers (Zyskin et al., 1981).

Hence the UV fraction in Čerenkov light at observation level is a useful parameter. We estimated this fraction for primaries of various energies. We divided the Čerenkov photon spectrum as seen at the observation level into two groups

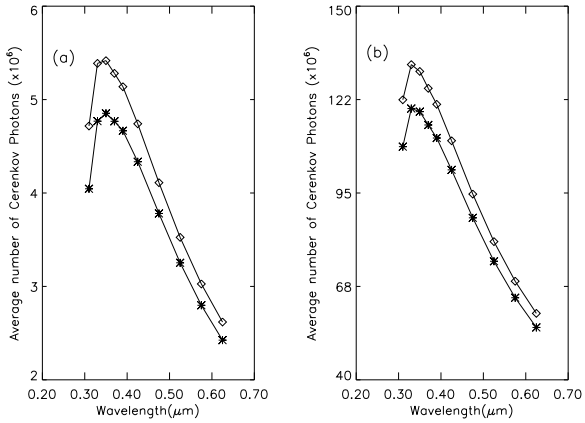

Fig. 4. Typical Čerenkov photon spectra at Pachmarhi level. (a) Spectra from $\gamma-$ray primaries of energy 50 GeV and 100 GeV protons (b) Spectra for 1 TeV $\gamma-$ray & 2 TeV proton primaries. The symbols used are * for $\gamma-$rays and $\diamond$ for protons.

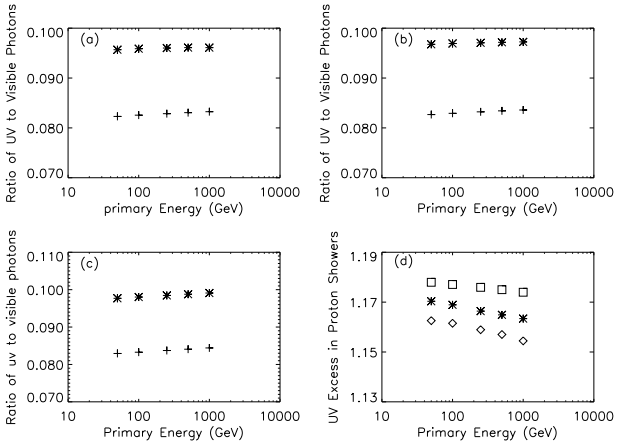

Fig. 5. Ratio of UV to visible fraction in Čerenkov light generated by protons (*) and $\gamma-$rays (+) *vs* primary energy, at three observation levels: (a) sea level (b) Pachmarhi and (c) 2 km a.s.l. (d) The relative excess in the UV content in hadronic primaries *vs* primary energy at three observation levels, in increasing order.

$viz.$, the UV range comprising wavelengths 270-300 nm and the visible range comprising the wavelength band 300-550 nm. The ratio of the number of photons in the UV range to that in the visible range is defined as R_p for proton primaries and R_γ for $\gamma-$ray primaries. Figure 5 shows a plot of R_p and R_γ as a function of primary energy for three different observation levels. Also shown in Figure 5 are the relative excess of UV content in proton showers *vis-a-vis* $\gamma-$ray showers, as a function of primary energy at three different altitudes.

5 Conclusions

In spite of the complexity of the interaction kinematics of high energy cosmic rays in the atmosphere, the average behavior as derived from simulations agrees reasonably well with analytical calculations. This demonstrates that the simulation package does take into account almost all the interaction characteristics giving credence to the conclusions drawn from simulations. We have derived incident photon spectra generated by $\gamma-$ray and hadronic primaries at various observation altitudes by applying wavelength dependent corrections due to photon attenuation in the atmosphere during propagation of photons to observation level. The incident photon spectra are found to be both altitude and energy dependent with the peak of the spectrum shifting towards shorter wavelength for increasing altitude or energy. We have also estimated the fraction of UV component of incident spectra for both the species at various observation altitudes. Hadron generated Čerenkov spectra are found to be richer in UV light at higher altitudes. Also the relative strength of UV increases at higher primary energies. For example, the relative strength of UV photons to the visible is higher in the case of proton primaries by about 16% at 50 GeV and decreases to 12% at 1 TeV. Hence, the hadron discrimination efficiency based on the UV content in Čerenkov light is relatively better at lower primary energies and at near core distances. Thus, measurement of relative UV content of a shower could be a good parameter in order to discriminate against hadrons especially for large ground based arrays with low energy thresholds ($\sim 20 - 50\ GeV$). However for this technique to be successful one has to make a very accurate (better than $\sim 1\%$) estimate of the UV and visible light contents of the shower.

References

Chitnis, V. R. and Bhat, P. N., Astropart. Phys., 9, 45, 1998.

Chitnis, V. R. *et al.*, 'Pachmarhi Array of Čerenkov Telescopes and its sensitivity', these proceedings, 2001.

Elterman, L., US Airforce Cambridge Research Laboratory Report AFCRL-68-0153, 1968.

Gaisser, T. K. and Hillas, A. M., Proc. 14^{th} ICRC, Plovdiv, 8, 353, 1977.

Goret, P., et al., Nucl. Inst. Meth., A270, 550, 1988.

Greisen, K., Prog. in Cosmic Rays Phys., 3, 1, 1956.

Heck, D. *et al.*, Forschungszentrum Karlsruhe Report, FZKA 6019, 1998.

Lythe, G. D., Search for high energy gamma rays from 1987A, JANZOS Collaboration, ICRR, Univ. of Tokyo, 362-368, 1990

Ong, R., *Phys. Rep.*, 305, 93, 1998.

Pyrke, C. L., Astro-ph Preprint Archive, astro-ph/0003442, 2000.

Rahman, M. A. et al., to appear in Experimental Astronomy, astro-ph/0104143, 2001.

Rao, M. V. S. and Sreekantan, B. V., Extensive Air Showers, Tata McGraw Hill, 23-24, 1998.

Zatsepin, V. I. and Chudakov, A. E., Sov Phys.-JETP, 15, 1126, 1962. 1981.

Zyskin, Yu. L. et al., Proc. 20^{th} ICRC, Moscow, 2, 342, 1981.